

# QUANTIFYING THE RESPONSE OF BLAINVILLE’S BEAKED WHALES TO U.S. NAVAL SONAR EXERCISES IN HAWAII

Eiren K. Jacobson<sup>1\*</sup>, E. Elizabeth Henderson<sup>2</sup>, Cornelia S. Oedekoven<sup>1</sup>, David  
L. Miller<sup>1</sup>, Stephanie L. Watwood<sup>3</sup>, David J. Moretti<sup>3</sup>, Len Thomas<sup>1</sup>

<sup>1</sup> *Centre for Research into Ecological and Environmental Modelling, University of St Andrews, St  
Andrews, Scotland, UK*

<sup>2</sup> *Naval Information Warfare Center Pacific, San Diego, CA, USA*

<sup>3</sup> *Naval Undersea Warfare Center, Newport, RI, USA*

Corresponding author (email: eiren.jacobson@st-andrews.ac.uk)

Draft 09 January 2020

## Abstract

Naval use of mid-frequency active (MFA) sonar has been associated with injury and death of multiple species of marine mammals. Deep-diving beaked whales (family Ziphiidae) are particularly susceptible to naval sonar. The US Navy operates multiple training and testing facilities where MFA sonar is used regularly, and where cumulative sublethal impacts of exposure to MFA sonar could have negative effects on beaked whale populations. Our goal was to quantify the response of Blainville’s beaked whales (*Mesoplodon densirostris*) to sonar on the Pacific Missile Range Facility (PMRF) in Hawaii. One indicator of a behavioral response to MFA sonar is reduced foraging activity. In the present study, we use data on Blainville’s beaked whale foraging activity collected at bottom-mounted hydrophones before and during six Naval sonar exercises.

## 1 Introduction

Beaked whales (family Ziphiidae) are a group of deep-diving cetaceans that rely on sound to forage, navigate, and communicate (Aguilar de Soto et al., 2012; Johnson, Madsen, Zimmer, Aguilar de Soto, and Tyack, 2004; Macleod and D’Amico, 2006). Multiple mass strandings of beaked whales have been associated with high-intensity anthropogenic sound sources. These acute events have motivated research into whether and how beaked whales respond to different types and intensities of anthropogenic noise (Cox et al., 2006).

Anthropogenic sound can disrupt the patterned dive cycles of these animals [CITE e.g. Falcone, also Southall re synchronicity?], potentially leading to death [CITE Jepson] or to cumulative sublethal impacts [PCoD, CITE]. For example, research on Blainville’s beaked whales *Mesoplodon densirostris* on a Navy range in the Bahamas has shown that animals may stop foraging and/or move away from sonar sources (Joyce et al., 2019; Tyack et al., 2011).

Naval sonar can be broadcast from various platforms, including vessels, helicopters, buoys, submarines, and autonomous vehicles (or should this say torpedoes?) (CITE?). Most research has focused on the impacts of mid-frequency active (MFA) sonar broadcast from Naval vessels, but has not been able to isolate the effect of the Naval vessels themselves. Separately, researchers have shown that, in the absence of MFA sonar, beaked whales may alter their behavior in response to vessel noise (Aguilar Soto et al., 2006; Pirodda et al., 2012).

There are different experimental and analytical ways of quantifying responses to sonar. Here, we focus on methods used for analysis of data from cabled hydrophone arrays.

For example, (McCarthy et al., 2011) used separate GAMS for before/during/after, response was GVPs per 5 hr periods, explanatory vars were inner/outer and time. Hypotheses were evaluated using z-tests.

(Moretti et al., 2014) used a GAM to model dive presence/absence as a function of a smooth on sonar RL. They and compared the predicted probability of dive presence at varying RLs to a baseline calculated from pre-sonar data to calculate the probability of disturbance.

In the present study, we wanted to look at cumulative effects of Naval training activity and MFA sonar while explicitly accounting for differences in underlying beaked whale presence. We wanted to isolate the effect of training activity from the effect of hull-mounted MFA sonar. To do this, we used a spatially referenced dataset of Blainville’s beaked whales from Hawaii. Data were collected via a cabled hydrophone array before and during six Naval training exercises. Previous work in this region has shown that Blainville’s beaked whales are present year-round at this site, that they prefer certain slope habitats, and that acoustic detections decrease during multi-day training events (Henderson, Martin, Manzano-Roth, and Matsuyama, 2016; Manzano-Roth, Henderson, Martin, Martin, and Matsuyama, 2016).

Here, we . . .

## 2 Methods

### 2.1 Acoustic detection of beaked whales

The Pacific Missile Range Facility (PMRF) is an instrumented U.S. Naval range extending 70 km NW of the island of Kauai, Hawaii and encompassing 2,800 km<sup>2</sup>. The range includes a cabled hydrophone array (Fig. 1) with hydrophones at depths ranging from approximately 650 m to 4,700 m. HYDROPHONE SPECS HERE. Up to 64 of the range hydrophones can be recorded simultaneously by the Naval Information Warfare Center (NIWC). Data are digitized at a rate of XXX samples/sec. DETAILS OF BEAKED WHALE DETECTION

ALGORITHM HERE. An automated routine (CITE) is used to group detections of individual beaked whale echolocation clicks into Group Vocal Periods (GVPs). If a group of whales is detected by more than one hydrophone, the GVP is assigned to the hydrophone that recorded the most clicks. The data are then aggregated to indicate presence or absence of beaked whale group(s) for each hydrophone within each half-hour period. In the present study, we used data collected before and during Submarine Commander Courses (SCCs) at the PMRF. SCCs occur biannually in February and August. SCCs typically last X days, and NIWC records for a minimum of 2 days before each SCC.

## 2.2 Modelling received levels of hull-mounted mid-frequency active sonar

NIWC receives logs of all ship and other activity that occurs on the range during each SCC. The ship logs indicate the locations of the ships during the training periods and also indicate the start and stop times of each individual training event, but no information is provided on the start and stop of sonar use. NIWC uses sonar detections within the acoustic data to determine periods of active sonar. Using the logs, the locations of all ships are noted for each half-hour period and the closest ship to each hydrophone is determined. Propagation modelling is used to calculate the expected received level of hull-mounted mid-frequency active sonar at each hydrophone from the closest ship during each half-hour period of each SCC. The propagation modelling is done within the program Peregrine (CITE), which uses a parabolic equation to estimate the transmission loss between the ship and the hydrophone, which is converted to a received level at the hydrophone based on the source level of the sonar. Transmission loss is estimated using a 200 Hz band around the center frequency of the sonar type (here, 35 kHz). Transmission loss is estimated at depth; for hydrophones shallower than 1000 m the received level is estimated at a point 20 m above the sea floor, while for hydrophones deeper than 1000 m the received level is estimated at 1000 m depth. The maximum received level was determined for each hydrophone and half-hour period and aggregated with the data on beaked whale group detections. Uncertainty in the modelled received level was not considered.

## 2.3 Spatial Modelling

Modelling methods are described in detail in the following sections. Briefly, we first used a tessellation to determine the area effectively monitored by each hydrophone. Then, we used pre-activity data to create a spatial model of the probability of GVPs prior to the onset of Naval activity. We used the predicted values from this model as an offset in a model created using data from when Naval activity was present on the range, but MFA sonar was not. Again, we used the predicted values from this model as an offset in a model created using data when Naval activity and MFA sonar were present on the range. Finally, we used posterior simulation to calculate confidence intervals and quantified the change in the probability of GVPs when Naval activity was present and across received levels of MFA sonar.

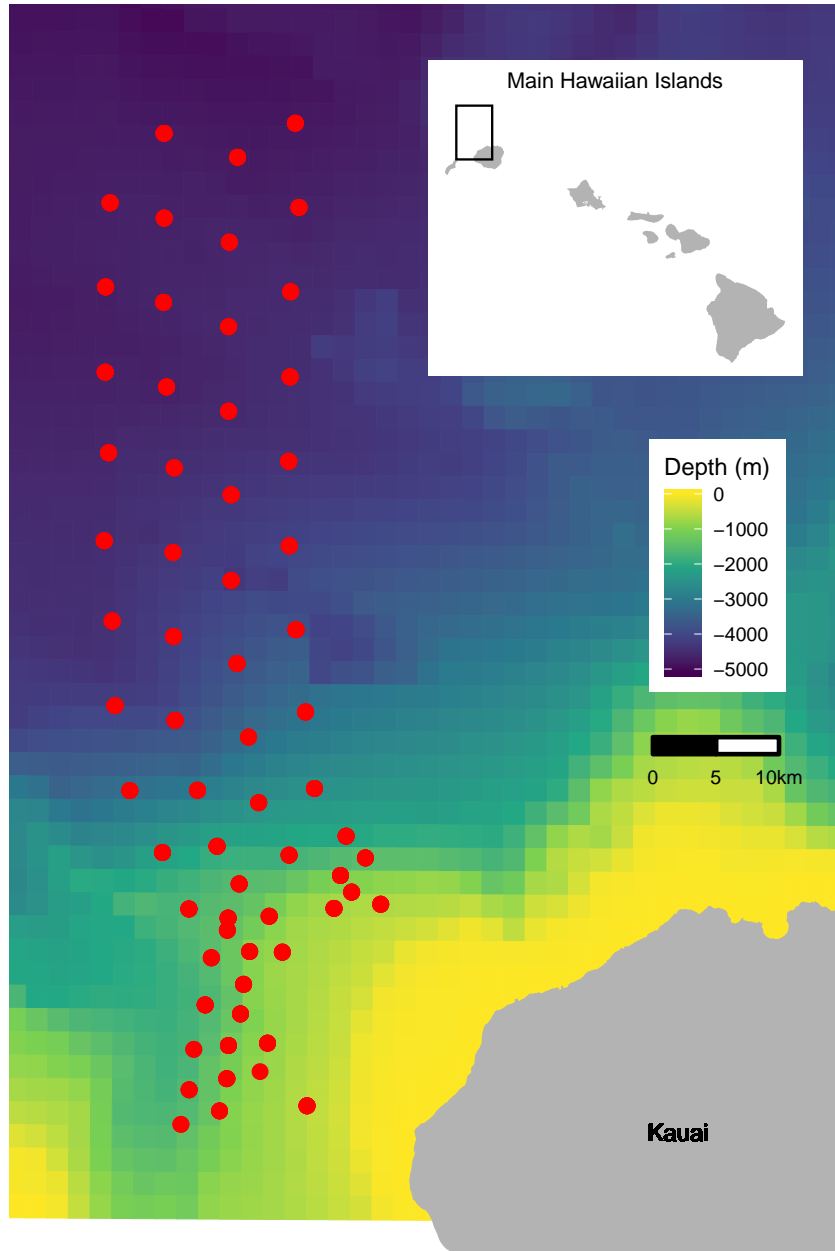


Figure 1: Map of approximate locations of hydrophones (red points) at the Pacific Missile Range Facility. Inset map shows range location relative to the Main Hawaiian Islands.

### 2.3.1 Determining hydrophone effort

For security reasons, randomly “jittered” locations and depths of hydrophones at PMRF were used. The hydrophone locations were jittered by up to XX m and depths were jittered by up to XX m. We projected the coordinates of each hydrophone into Universal Transverse Mercator Zone 4.

Because the beaked whale detection algorithm assigns groups of whales to the hydrophone that recorded the most echolocation clicks, and because the spatial separation of the hydrophones is not uniform, effort is not the same for all hydrophones. To determine the area effectively monitored by each hydrophone, we used a Voronoi tessellation implemented in the R (R Core Team, 2018) package `deldir` (Turner, 2019) to define a tile for each hydrophone that contained all points on the range that were closest to that hydrophone. The area of each tile corresponds to the effective area monitored. We assume that beaked whale groups occur within the tessellation tile of the hydrophone to which the GVP is assigned. For hydrophones on the outside of the range, i.e., not surrounded by other hydrophones, we used a cutoff radius of 6500 m to bound the tessellation tile. This distance is based on the maximum detection distance of individual Blainville’s beaked whale clicks at a U.S. Naval range in the Bahamas (T. A. Marques, Thomas, Ward, DiMarzio, and Tyack, 2009). Different combinations of hydrophones were used during different SCCs, so separate tessellations were created for each SCC.

### 2.3.2 M1: Modelling the pre-activity probability of dive detection

We used data collected prior to SCCs, when no Naval ships were present on the range and no other Naval activity was known to occur, to determine the baseline probability of GVPs at each hydrophone. The exact locations of beaked whale groups is not known; rather, detections of beaked whale groups are “snapped” to hydrophone locations depending on which hydrophone detected the most echolocation clicks. Therefore, the data are not continuous in space. To account for this, we used a Markov random field to model the spatial distribution of GVPs. A Markov random field (Rue and Held, 2005) is a method for modelling correlation in space between discrete spatial units. Each unit is correlated more strongly with its neighbours (those units which touch) than those that are more hops away. This gives a graph-like structure, where “number of hops” is the distance used to calculate relatedness, rather than geographical distance. This is appropriate for our data as we do not know where in each tile a given GVP occurs, but we assume that it does occur in that tile.

The R package `mgcv` (Wood, Li, Shaddick, and Augustin, 2017) was used to formulate the model on the tessellation described in the previous section. The linear predictor for the model was:

$$\text{logit}(\mu_{\mathbf{M1},i}) = \beta_{\mathbf{M1},0} + f(\mathbf{MRF}_i) + f(\text{Depth}_i) + \log_e A_i, \quad (\mathbf{M1}) \quad (1)$$

where  $\text{DivePresent}_i \sim \text{Bin}(1, \mu_{\mathbf{M1},i})$ . The spatial smooth MRF is given by  $f(\mathbf{MRF}_i)$ ,  $f(\text{Depth}_i)$  is a smooth of depth (using a thin plate spline) and  $\log_e A_i$  is an offset for the area (in

km<sup>2</sup>) of each tile,  $A_i$ . The offset term accounts changes in probabilities of detection due to the differing area monitored per hydrophones. Because the hydrophone tessellations change between SCCs, separate MRFs were used for each SCC, but a single smoothing parameter was estimated across all MRFs. Therefore different spatial patterns could occur, but with the same amount of variation. The smooth of depth was shared across SCCs.

NOTE:  $f(\text{MRF})$  could be indexed by SCC to indicate that the smooth function is different for each.

### 2.3.3 M2: Modelling the effect of Naval activity

For a few days prior to the onset of hull-mounted MFA sonar used during SCCs, Naval training activities occur at the PMRF. Ships are present on the range during this period and other noise sources, including live-fire and submarines, may be present. We used data collected when ships were present on the range, but hull-mounted MFA sonar was not used, to model the effect of general Naval activity on beaked whale GVPs. Initially, we tried to use low-frequency noise levels measured on range hydrophones as a covariate in this model, but found that the measured noise levels were not consistent with known locations of Naval training activities (see Appendix B for details).

We used the predicted baseline probability of a GVP from Model 1 as an offset to control for the underlying spatial distribution of GVPs. The model for the data when ships were present was intercept-only, with an offset derived from M1. This model was simply:

$$\text{logit}(\mu_{\text{M2},i}) = \beta_{\text{M2},0} + \log_e \xi_{\text{M1},i}, \quad (\text{M2}) \quad (2)$$

where  $\text{DivePresent}_i \sim \text{Bin}(1, \mu_{\text{M2},i})$ .  $\xi_{\text{M1},i}$  denotes the prediction (on the logit scale) for tile  $i$  using model M1. This was again modelled in the R package `mgcv`.

### 2.3.4 M3: Modelling the effect of hull-mounted MFA sonar

We used data collected when hull-mounted MFA sonar was present on the range to model the effect of sonar on beaked whales. The probability of a dive when sonar was present was modelled as a function of the maximum received level (modelled at each hydrophone; see section 2.2). We assumed that as the maximum received level increased, the probability of dives decreased and modelled this using a shape constrained smooth so that the relationship held for all possible realizations of the smooth. To ensure that the model predictions were the same at a maximum received level of 0 dB and when ships were not present, we did not include an intercept. This model was written as:

$$\text{logit}(\mu_{\text{M3},i}) = f(\text{MaxRL}_i) + \log_e \xi_{\text{M2},i}, \quad (\text{M3}) \quad (3)$$

where  $\text{DivePresent}_i \sim \text{Bin}(1, \mu_{\text{M3},i})$ .  $f(\text{MaxRL}_i)$  was modelled as a monotonic decreasing smooth using the R package `scam` (Pya and Wood, 2015).  $\xi_{\text{M2},i}$  denotes the prediction (on the logit scale) for tile  $i$  when Naval training activities were present on the range using model M2.

### 2.3.5 Uncertainty propagation

We used posterior simulation to propagate uncertainty through M1, M2, and M3. Each model was fitted via restricted maximum likelihood (REML; Wood, 2008), so the results are empirical Bayes estimates. In this case we can generate samples from the (multivariate normal) posterior of the model parameters. After generating a sample,  $\beta^* \sim \text{MVN}(\hat{\beta}, \mathbf{V}_\beta)$ , we can use the matrix that maps the model parameters to the predictions on the linear predictor scale [often referred to as the  $\mathbf{L}_p$  matrix or  $\mathbf{X}_p$  matrix; Wood et al. (2017); section 7.2.6], along with the inverse link function to generate predictions for each posterior sample. Here the  $\beta$  for each model includes the coefficients for the smooth terms in the model and fixed effects (e.g., intercept) if present. Predictions,  $\mu^*$ , can be written as:

$$\mu^* = g^{-1}(\eta^*) = g^{-1}(\mathbf{X}_p \beta^* + \xi), \quad (4)$$

where  $g$  is the link function,  $\eta^*$  is the linear predictor and  $\xi$  is any offset used by this prediction. By sampling from the posterior of  $\hat{\beta}$ , and then taking the variance of the resulting  $\mathbf{p}^*$ s we can obtain variance estimates [Wood et al. (2017); section 7.2.6]. The prediction grid contained all possible combinations of covariates within the realized covariate space; i.e., each hydrophone for each SCC with associated location, hydrophone depth, and area of the tessellation tile, presence/absence of Naval activity, and, if Naval activity present, then either sonar absence or sonar received level between 35 and 190 dB in intervals of 5 dB.

This procedure needs to happen for each model, updating the offsets and refitting as it goes.

An algorithm for calculating the variance from our multi-stage approach is as follows. First define  $N_b$  as the number of samples to make, let  $\mathbf{X}_{p,\text{M}j}$  for  $j = 1, 2, 3$  be the  $\mathbf{L}_p$  matrix that maps coefficients to the predictions for model  $\text{M}j$ . For  $N_b$  times:

1. Draw a sample from the posterior of M1:  $\tilde{\beta}_{\text{M1}} \sim \text{MVN}(\hat{\beta}_{\text{M1}}, \mathbf{V}_{\text{M1}})$ .
2. Calculate a new offset for M2,  $\tilde{\xi}_{\text{M1}} = \mathbf{X}_{p,\text{M1}} \tilde{\beta}_{\text{M1}} + \log_e \mathbf{A}$ .
3. Refit M2 with  $\tilde{\xi}_{\text{M1}}$  as the offset, to obtain M2'.
4. Draw a sample from the posterior of M2':  $\tilde{\beta}_{\text{M2}'} \sim \text{MVN}(\hat{\beta}_{\text{M2}'}, \mathbf{V}_{\text{M2}'})$
5. Calculate a new offset for M3,  $\tilde{\xi}_{\text{M2}} = \mathbf{X}_{p,\text{M2}} \tilde{\beta}_{\text{M2}'} + \tilde{\xi}_{\text{M1}}$  (predictions for the sonar data locations for M2').
6. Refit M3 with offset  $\tilde{\xi}_{\text{M2}}$  to obtain M3'.
7. Predict  $\mu_{\text{M1}'}$ ,  $\mu_{\text{M2}'}$ , and  $\mu_{\text{M3}'}$  over prediction grid and store them.

208 We can then calculate summary statistics (means and variances) of the  $N_b$  values of  $\mu_{M1'}$ ,  
 209  $\mu_{M2'}$ , and  $\mu_{M3'}$  we have generated. The empirical variance of the  $N_b$  values of  $\mu_{M3'}$  will give  
 210 the uncertainty, incorporating components from all three models. We can take appropriate  
 211 quantiles to form confidence intervals for the functional relationships between [TKTKTK  
 212 noisy boi] and [TKTKTK whaley boi].

### 213 2.3.6 Quantifying the change in probability of GVPs

214 Finally, we calculated the expected change in the probability of GVPs relative to either the  
 215 distribution of GVPs when no general Naval training activity was present and no MFA sonar  
 216 was present ( $\Delta_{M3':M1'}$ ), or relative to the distribution of GVPs general Naval training activity  
 217 was present but no MFA sonar was present ( $\Delta_{M3':M2'}$ ).

218 Using the  $N_b$  bootstrapped model realizations we calculated the expected probability of a  
 219 GVP under each set of covariates as

$$\mathbb{P}(\text{GVP}) = \text{logit}^{-1}(\mu_{\mathbf{M}}), \quad (5)$$

220 for each  $M1'$ ,  $M2'$ , and  $M3'$ . Then, we calculated the change in  $\mathbb{P}(\text{GVP})$  for each set of  
 221 covariates  $M3'$  and  $M1'$  ( $\Delta_{M3':M1'}$ ) and between  $M3'$  and  $M2'$  ( $\Delta_{M3':M2'}$ ) for each realization of  
 222 the bootstrap.

$$\Delta_{M3':M1'} = \frac{\mathbb{P}(\text{GVP})_{M3'} - \mathbb{P}(\text{GVP})_{M1'}}{\mathbb{P}(\text{GVP})_{M1'}} \quad (6)$$

$$\Delta_{M3':M2'} = \frac{\mathbb{P}(\text{GVP})_{M3'} - \mathbb{P}(\text{GVP})_{M2'}}{\mathbb{P}(\text{GVP})_{M2'}} \quad (7)$$

223 For each received level we calculated the 2.5th, 50th, and 97.5th quantiles of  $\Delta_{M3':M1'}$  and  
 224  $\Delta_{M3':M2'}$  to create 95% CIs of change in  $\mathbb{P}(\text{GVP})$  across possible received levels. We consider  
 225 that the probability of disturbance is equal to 1 wherever the 95% CI does not include 0, and  
 226 0 otherwise.

## 227 3 Results

228 Data were collected before and during six SCCs; two each in in 2013, 2014, and 2017 (Table  
 229 1). The number of hydrophones for which recordings were available varied from 49 to 61. A  
 230 total of 190928 30-min observations were made.



Table 1: No. of hydrophones used and number of observations made (no. 30-min periods) for each SCC before the exercise began, when Naval activity was present, and when Naval activity and MFA sonar were present.

SCC	HPs	Pre-Activity	Nav. Activity	MFA Sonar
Feb13	61	114	193	124
Aug13	61	209	115	97
Feb14	60	513	111	129
Aug14	61	263	120	128
Feb17	59	450	97	108
Aug17	49	270	106	113

The exact timing of activities during these exercises varied (Fig. 2). For most SCCs, pre-activity data were available immediately preceding the onset of Naval training activity; however, in February 2013 the only available pre-activity data were collected more than a month prior to the onset of Naval training activity. In some SCCs, weekends or other breaks in training resulted in absence of Naval ships on the range during the days preceding MFA sonar use. MFA sonar was used for 3-4 days during each training event.

Across all SCCs, hydrophones, and conditions, a total of 2312 GVPs were identified. The average probability of a GVP in the dataset was therefore 1%. The spatial distribution of GVPs differed during the pre-activity phases of SCCs (Fig. SX; top panel).

Modelled maximum received levels ranged from 38 to 186 dB re.  $1 \mu$  Pa, with a median value when MFA sonar was present of 147 dB re.  $1 \mu$  Pa. The intensity and spatial distribution of MFA received levels varied across the range and across SCCs (Fig. SX).

Based on the observed data, the probability of a GVP within a 30-min period changed by -57% when Naval activity was present compared to when Naval activity was absent, by -47% when Naval activity and MFA sonar were present compared to when only ships were present, and by -77% when Naval activity and MFA sonar were present compared to when neither ships nor sonar were present (Fig. S2).

## 3.2 Results of spatial modelling

We created separate tessellations for each SCC (Fig. SX). In August 2017, data were available from fewer hydrophones, and so in some cases the tessellated tiles, with bounding radius of 6500 m, did not completely cover the range.

Hydrophone depths varied from 648 to 4716 m. The model M1 predicted highest probability of GVPs at hydrophone depths between 1500 and 2000 m, consistent with other findings that Blainville’s beaked whales prefer to forage in slope habitats [CITE].

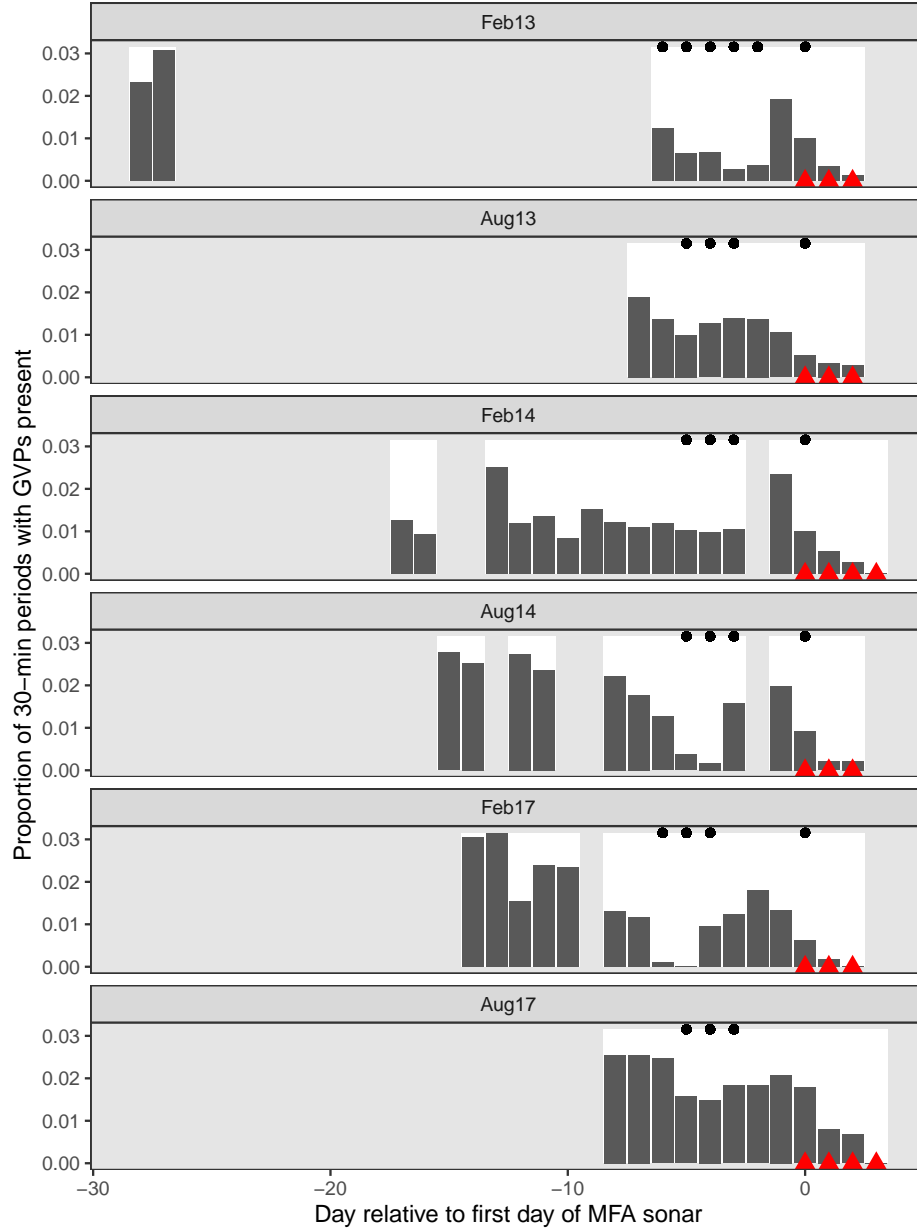


Figure 2: Timeseries of six recorded Naval training activities at PMRF. The timeseries are aligned relative to the first day that MFA sonar (red triangles) was used in each exercise (x-axis). Days with white background indicate days for which recordings and data were available. Gray bars indicate the proportion of 30-min periods on each day, across all hydrophones, when GVPs were detected. Black dots indicate days when Naval activity was present on the range.

M2 used the predicted values from M1 as an offset and fitted a model to data when Naval activity was ongoing, as indicated by the presence of ships.

- M3 (spline on MaxRL, could reinstate 3-panel figure with dots or line for each HP?)
- Uncertainty prop
- Total change

## 4 Discussion

- Describe why we didn't use a single giant GAM – didn't want contamination of the baseline period by the spatial distribution of sonar, would lead to underestimates of the impact of sonar. Could present the single giant GAM in an appendix.
- Discuss unusual timeline of Feb13
- Discuss what “Naval activity” could mean
- GVPs appear to decrease over the course of MFA sonar; this is something we could investigate with a spatio-temporal model in the future (hour since onset of MFA? SEL?)
- Discuss dose-response and p(disturbance) in context of (Tyack and Thomas, 2019)

## References

- Aguilar de Soto, N., Madsen, P. T., Tyack, P., Arranz, P., Marrero, J., Fais, A., ... Johnson, M. (2012). No shallow talk: Cryptic strategy in the vocal communication of Blainville's beaked whales. *Marine Mammal Science*, 28(2), E75–E92. <https://doi.org/10.1111/j.1748-7692.2011.00495.x>
- Aguilar Soto, N., Johnson, M., Madsen, P. T., Tyack, P. L., Bocconcelli, A., & Fabrizio Borsani, J. (2006). DOES INTENSE SHIP NOISE DISRUPT FORAGING IN DEEP-DIVING CUVIER'S BEAKED WHALES (ZIPHIUS CAVIROSTRIS)? *Marine Mammal Science*, 22(3), 690–699. <https://doi.org/10.1111/j.1748-7692.2006.00044.x>
- Cox, T., Ragen, T., Read, A., Vos, E., Baird, R., Balcomb, K., ... others. (2006). Understanding the impacts of anthropogenic sound on beaked whales1. *J. CETACEAN RES. MANAGE*, 7(3), 177–187.
- Henderson, E. E., Martin, S. W., Manzano-Roth, R., & Matsuyama, B. M. (2016). Occurrence and Habitat Use of Foraging Blainville's Beaked Whales (*Mesoplodon densirostris*) on a U.S. Navy Range in Hawaii. *Aquatic Mammals*, 42(4), 549–562. <https://doi.org/10.1578/AM.42.4.2016.549>
- Johnson, M., Madsen, P. T., Zimmer, W. M. X., Aguilar de Soto, N., & Tyack, P. L. (2004).

Beaked whales echolocate on prey. *Proceedings of the Royal Society of London. Series B: Biological Sciences*, 271(suppl\_6). <https://doi.org/10.1098/rsbl.2004.0208>

Joyce, T. W., Durban, J. W., Claridge, D. E., Dunn, C. A., Hickmott, L. S., Fearnbach, H., ... Moretti, D. (2019). Behavioral responses of satellite tracked Blainville's beaked whales ( *Mesoplodon densirostris* ) to mid-frequency active sonar. *Marine Mammal Science*, mms.12624. <https://doi.org/10.1111/mms.12624>

Macleod, C. D., & D'Amico, A. (2006). *A review of beaked whale behaviour and ecology in relation to assessing and mitigating impacts of anthropogenic noise*. 11.

Manzano-Roth, R., Henderson, E. E., Martin, S. W., Martin, C., & Matsuyama, B. (2016). Impacts of U.S. Navy Training Events on Blainville's Beaked Whale (*Mesoplodon densirostris*) Foraging Dives in Hawaiian Waters. *Aquatic Mammals*, 42(4), 507–518. <https://doi.org/10.1578/AM.42.4.2016.507>

Marques, T. A., Thomas, L., Ward, J., DiMarzio, N., & Tyack, P. L. (2009). Estimating cetacean population density using fixed passive acoustic sensors: An example with Blainville's beaked whales. *The Journal of the Acoustical Society of America*, 125(4), 1982–1994. <https://doi.org/10.1121/1.3089590>

McCarthy, E., Moretti, D., Thomas, L., DiMarzio, N., Morrissey, R., Jarvis, S., ... Dilley, A. (2011). Changes in spatial and temporal distribution and vocal behavior of Blainville's beaked whales (*Mesoplodon densirostris*) during multiship exercises with mid-frequency sonar. *Marine Mammal Science*, 27(3), E206–E226. <https://doi.org/10.1111/j.1748-7692.2010.00457.x>

Moretti, D., Thomas, L., Marques, T., Harwood, J., Dilley, A., Neales, B., ... Morrissey, R. (2014). A Risk Function for Behavioral Disruption of Blainville's Beaked Whales (*Mesoplodon densirostris*) from Mid-Frequency Active Sonar. *PLoS ONE*, 9(1), e85064. <https://doi.org/10.1371/journal.pone.0085064>

Pirotta, E., Milor, R., Quick, N., Moretti, D., Di Marzio, N., Tyack, P., ... Hastie, G. (2012). Vessel Noise Affects Beaked Whale Behavior: Results of a Dedicated Acoustic Response Study. *PLoS ONE*, 7(8), e42535. <https://doi.org/10.1371/journal.pone.0042535>

Pya, N., & Wood, S. N. (2015). Shape constrained additive models. *Statistics and Computing*, 25(3), 543–559. <https://doi.org/10.1007/s11222-013-9448-7>

R Core Team. (2018). *R: A Language and Environment for Statistical Computing*. Retrieved from <https://www.R-project.org/>

Rue, H., & Held, L. (2005). *Gaussian Markov Random Fields: Theory and Applications*. London: Chapman & Hall.

Turner, R. (2019). *Deldir: Delaunay Triangulation and Dirichlet (Voronoi) Tessellation*. Retrieved from <https://CRAN.R-project.org/package=deldir>

Tyack, P. L., & Thomas, L. (2019). Using dose–response functions to improve calculations of the impact of anthropogenic noise. *Aquatic Conservation: Marine and Freshwater*

324 *Ecosystems*, 29(S1), 242–253. <https://doi.org/10.1002/aqc.3149>

325 Tyack, P. L., Zimmer, W. M. X., Moretti, D., Southall, B. L., Claridge, D. E., Durban, J.  
 326 W., ... Boyd, I. L. (2011). Beaked Whales Respond to Simulated and Actual Navy Sonar.  
 327 *PLoS ONE*, 6(3), e17009. <https://doi.org/10.1371/journal.pone.0017009>

328 Wood, S. N. (2008). Fast stable direct fitting and smoothness selection for generalized additive  
 329 models. *Journal of the Royal Statistical Society: Series B (Statistical Methodology)*, 70(3),  
 330 495–518.

331 Wood, S. N., Li, Z., Shaddick, G., & Augustin, N. H. (2017). Generalized Additive Models  
 332 for Gigadata: Modeling the U.K. Black Smoke Network Daily Data. *Journal of the*  
 333 *American Statistical Association*, 112(519), 1199–1210. [https://doi.org/10.1080/01621459.](https://doi.org/10.1080/01621459.2016.1195744)  
 334 2016.1195744

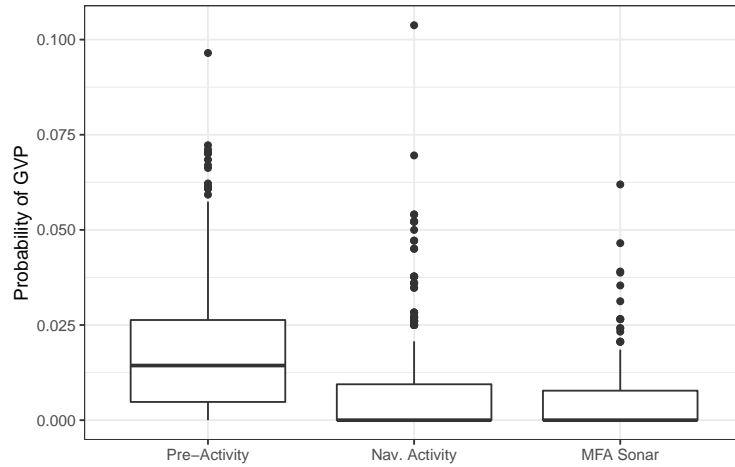
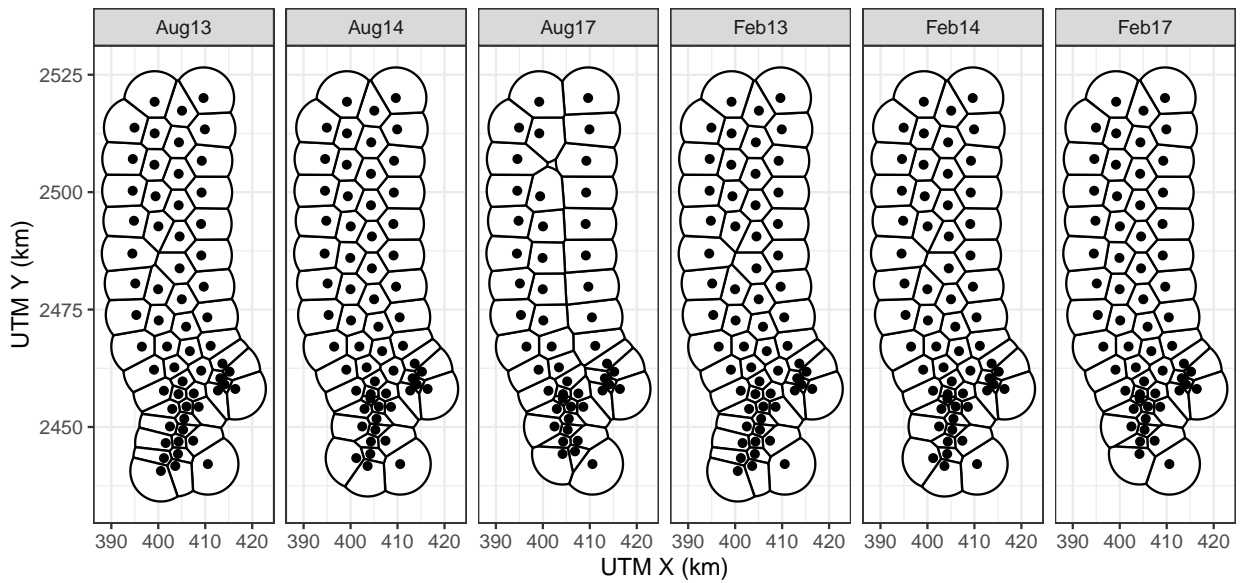


Figure 3: Boxplot of observed probability of diving across all hydrophones and SCCs before, when Naval activity was present, and when MFA sonar was present.

## Appendix A: Supplementary Tables and Figures



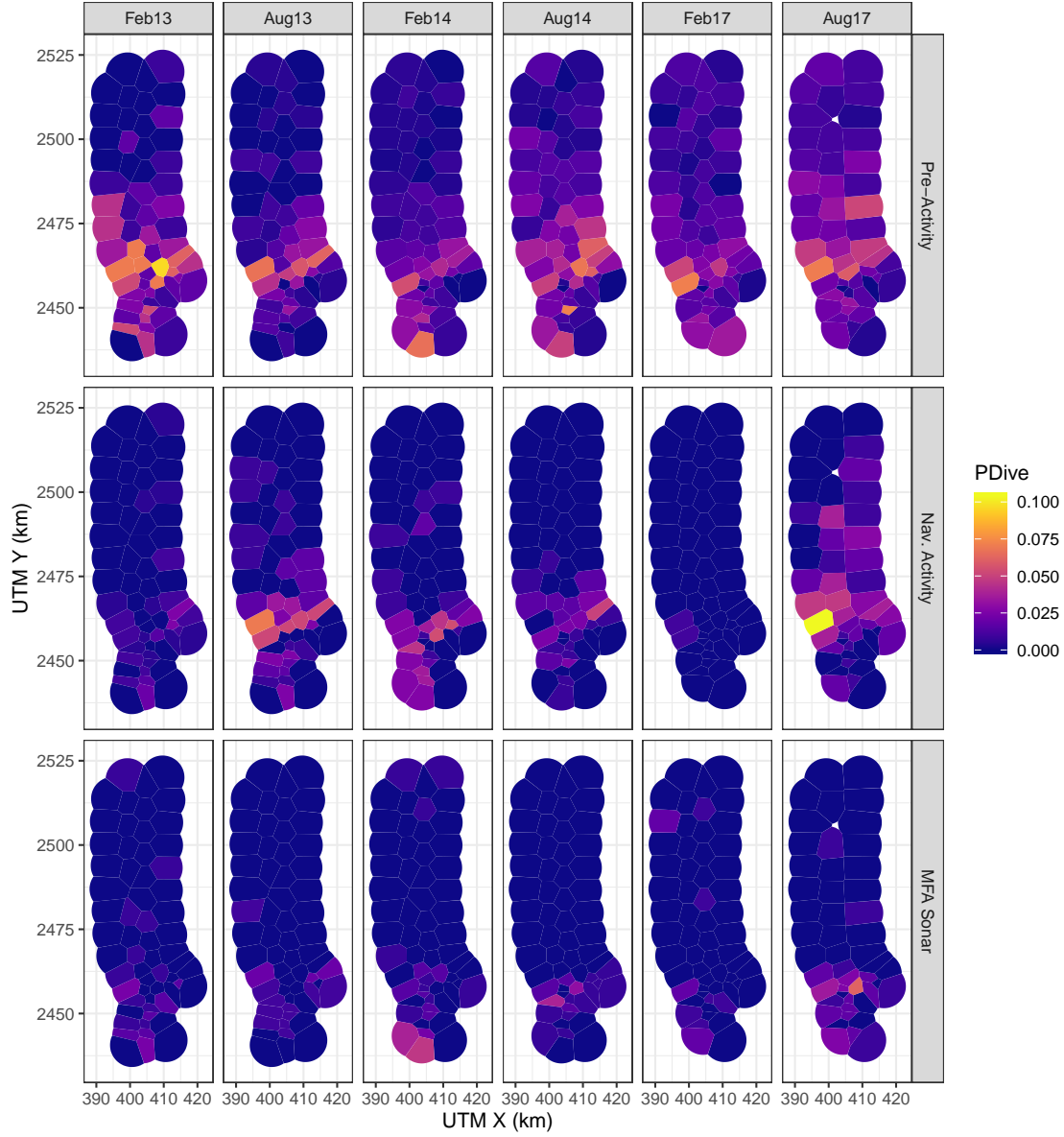


Figure 4: Map of observed probability of diving at each hydrophone before, during Phase A, and during Phase B of each SCC. Note that values of PDive are not corrected for effort (size of the hydrophone tile).

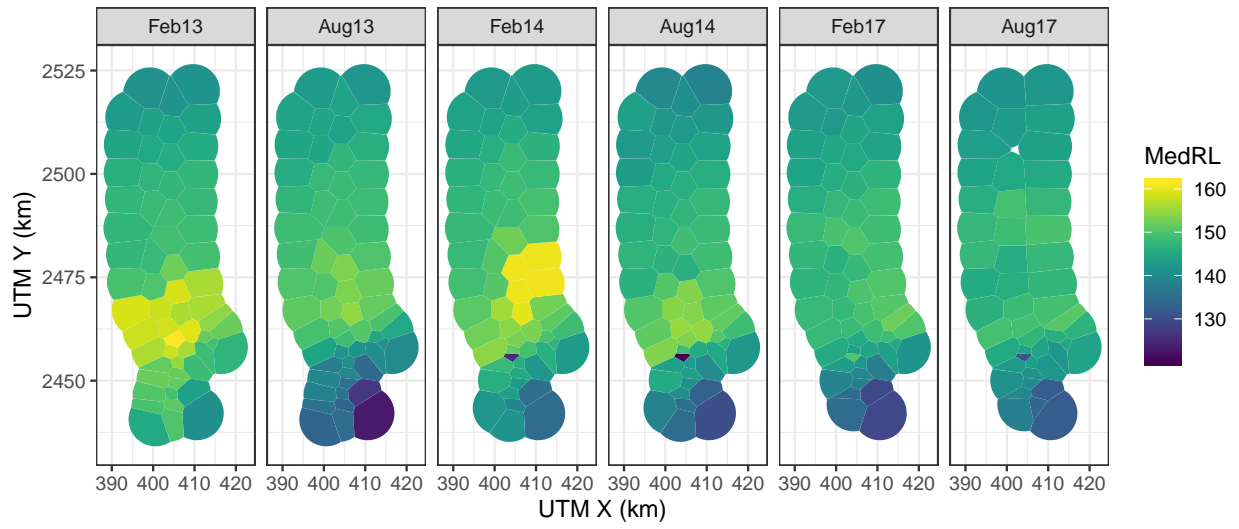


Figure 5: Median received level when MFA sonar was present (color scale) for all hydrophones and SCCs.